FULL PAPER

DOI: 10.1002/chem.200700897

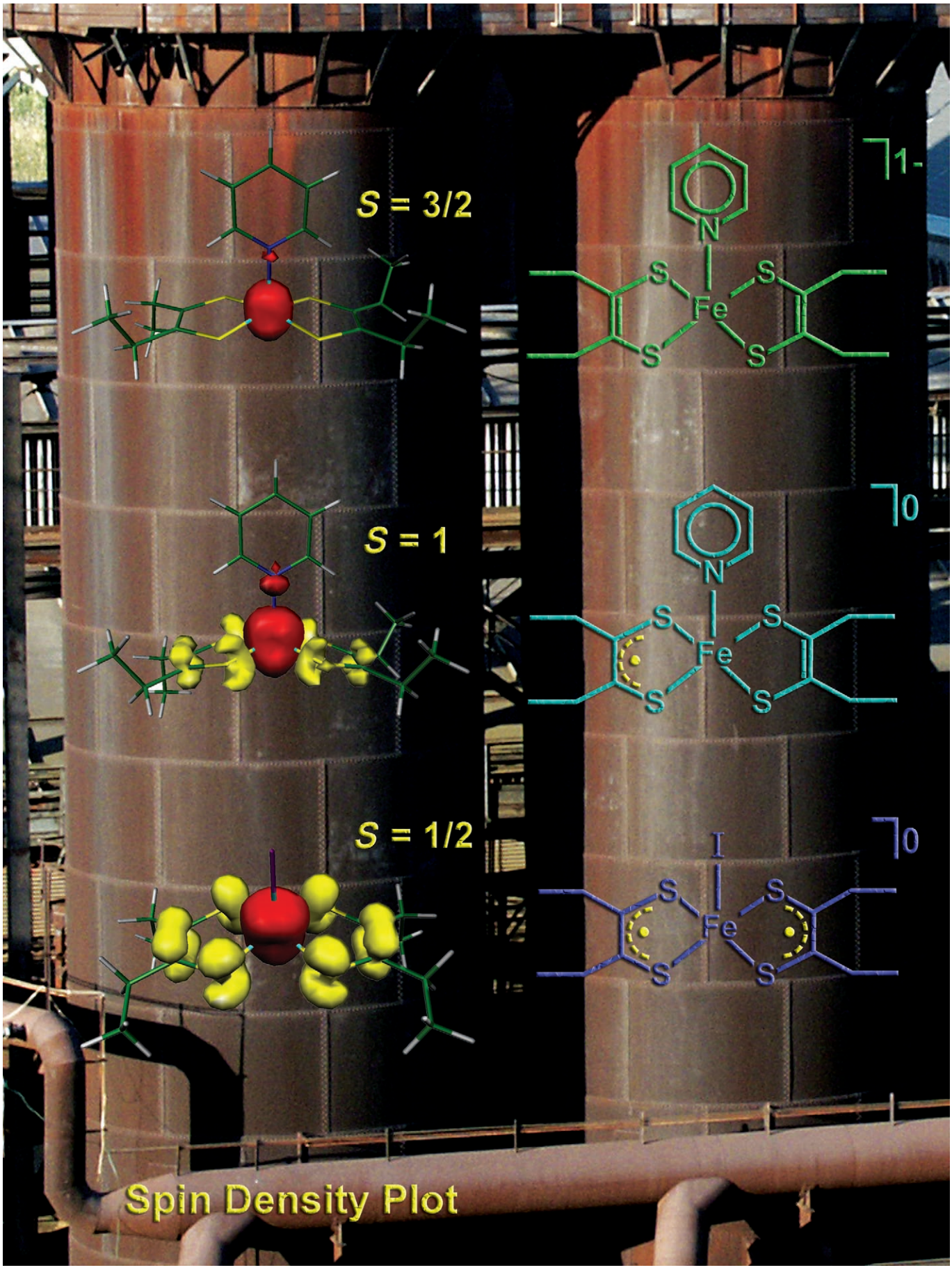

Electronic Structures of Five-Coordinate Complexes of Iron Containing Zero, One, or Two π-Radical Ligands: A Broken-Symmetry Density Functional Theoretical Study

Krzysztof Chłopek,[a] Nicoleta Muresan,[a] Frank Neese,*[b] and Karl Wieghardt*[a]

Dedicated to Professor Richard H. Holm

Abstract: The electronic structures of a series of five-coordinate complexes of iron containing zero, one, or two bidentate, organic π-radical ligands and a monodentate ligand (pyridine, iodide) have been studied by broken-symmetry (BS) density functional theoretical (DFT) methods. By analyzing the set of corresponding orbitals[5] (CO) a convenient division of the spin-up and spin-down orbitals into 1) essentially doubly-occupied molecular orbitals (MO), 2) exactly singly-occupied MOs, 3) spin-coupled pairs, and 4) virtual orbitals can be achieved and a clear picture of the spin coupling between the ligands (non-innocence vs. innocence) and the central metal ion (d^N configuration) can be generated. We have identified three classes of complexes which all contain a ferric ion (d^5) with an intrinsic intermediate spin ($S_{Fe}=3/2$) that yield 1) an $S_t=3/2$ ground spin state if the two bidentate ligands are closed-shell species (innocent ligands); 2) if one π-radical ligand is present, an $S_t=1$ ground state is obtained through intramolecular antiferromagnetic coupling; 3) if two such radicals are present, an $S_t=1/2$ ground state is obtained. We show unambiguously for the first time that the pentane-2,4-dione-bis(*S*-alkylisothiosemicarbazonato) ligand can bind as π-radical dianion $(L^{\bullet}_{TSC})^{2-}$ in $[Fe^{III}(L^{\bullet}_{TSC})I]$ ($S_t=1$) (**6**); the description as $[Fe^{IV}(L_{TSC}{}^{3-})I]$ is incorrect. Similarly, the diamagnetic monoanion in **14** must be described as $[Fe^{III}(CN)_2(L^{\bullet}_{TSC})]^-$ ($S_t=0$) with a low-spin ferric ion (d^5, $S_{Fe}=1/2$) coupled antiferromagnetically to a π-radical ligand; $[Fe^{II}(CN)_2(L_{TSC}{}^{-})]^-$ is an incorrect description.

Keywords: density functional calculations · intermediate spin · iron · ligand effects · radicals

Introduction

The evaluation of the correct valence electron count, the d^N configuration, for a given transition-metal coordination compound is an important task for the understanding (and prediction) of its spectroscopic properties and of its reactivity. The distinction between a *formal* oxidation (FOS) state and a *physical* oxidation (POS) has proven to be a highly useful concept.[1] The two oxidations states are commonly identical. However, they differ if one of the ligands in the complex is an open-shell, organic radical.[2] For example, in a complex containing an iron ion and a coordinated phenoxyl radical, for example, $[Fe(OH_2)_5(O^{\bullet}Ph)]^{3+}$, the FOS of the iron ion is +IV but the POS is +III. Non-innocent ligands[1] are often bound as open-shell π radicals. Therefore, the concept of redox (non)innocence of a given ligand can only be correctly used in conjunction with the POS of the metal center.[1] Note that the POS (that is the d^N configuration) has a clear connection to the interpretation of spectroscopic experiments as is well established from more than six decades of transition-metal optical and magnetic spectroscopy; the FOS, on the other hand, is a non-measurable number that is deduced by applying some simple rules (e.g., heterolytic bond cleavage between a closed-shell ligand and the metal ion[3]).

These radical ligand metal ion complexes, M–L$^{\bullet}$, constitute a fast growing class of coordination compounds. Identification of such a bonding situation experimentally is not at all simple, but the comparison of experimental and theo-

[a] Dr. K. Chłopek, Dr. N. Muresan, Prof. Dr. K. Wieghardt
Max-Planck-Institut für Bioanorganische Chemie
Stiftstrasse 34–36, 45470 Mülheim an der Ruhr (Germany)
Fax: (+49) 208-3063951
E-mail: wieghardt@mpi-muelheim.mpg.de

[b] Prof. Dr. F. Neese
Institut für Physikalische und Theoretische Chemie
Universität Bonn, Wegelerstr. 12, 53115 Bonn (Germany)
Fax: (+49)228-739064
E-mail: neese@thch.uni-bonn.de

Supporting information for this article is available on the WWW under http://www.chemeurj.org/ or from the author.

retically calculated (from density functional theory, DFT) spectroscopic properties has become a very valuable and efficient tool.[4] It should be realized that it is frequently not even straightforward to recognize in the calculations that the solution found corresponds, in fact, to a spin-coupled metal–radical system rather than to a classical Werner-type coordination compound. A safe indication that a nonstandard electronic structure has been found in the calculations is a spin-expectation value $\langle S^2 \rangle$ that deviates substantially from the value $S(S+1)$ predicted for a pure spin state (S is the total spin of the desired state). While such solutions are often disregarded as being simply "badly spin-contaminated", it should be realized that calculations based on Hartree–Fock (HF) or DFT theory are variational and that the variational principle makes a "desperate" attempt to describe a bonding situation for which the chosen single-determinant form of the HF or DFT wavefunction is not flexible enough. Thus, the electron density from such broken-symmetry (BS) DFT calculations is usually quite good, while spin-dependent properties and total energies require slight adjustments.

We have previously pointed out that considerable insight into the nature of the calculated bonding can be obtained by analyzing the so-called set of corresponding orbitals (COs).[5] Application of this transformation leads to a convenient division of the spin-up and spin-down orbital sets of a given spin-unrestricted solution to the HF or Kohn–Sham (KS) equations into four categories: 1) essentially doubly-occupied MOs, 2) exactly singly-occupied MOs, 3) spin-coupled pairs and 4) virtual orbitals. The spin-coupled pairs are formed by spin-up/spin-down pairs with a non-orthogonal spatial part—in the case of metal–radical interactions, one of the MOs is predominantly metal-centered and the partner orbital predominantly ligand-centered. The SOMOs and spin-coupled MOs can usually readily be identified with metal-d and ligand frontier orbitals. The strength of the interaction can be analyzed from the CO overlap (S_{ab}). In the limiting cases of $S_{ab} \rightarrow 1$ the system converges towards a standard, spin-(almost) pure solution, while for $S_{ab} \rightarrow 0$ an uncoupled system results.

Viewed in this way, the form of the BS-DFT wavefunction obtained by the CO transformation (COT) is, in fact, strongly reminiscent of Goddard's generalized valence bond (GVB) method[6]—a multiconfigurational ab initio method that has been applied with great success since the 1970 s. We refer to the COT in the framework of BS-DFT as "valence bond reading" of the electronic structure—the philosophy of such an approach has much in common with the early suggestions of Noodleman.[7]

In this paper we apply the BS DFT methodology to a number of five-coordinate complexes of iron which contain zero, one, or two π-radical ligands. The aim of the work is to elucidate computationally the electronic structures of complexes shown in Table 1; Scheme 1 shows the ligands used.

We will calibrate our theoretical approach to experiment by calculating the Mössbauer parameters[8] and compare these with experiment. In some cases we will show that the traditional, experimentally (spectroscopically) derived electronic structures are in fact incorrect and need to be revised.

Table 1. Electronic structures of complexes investigated in this paper.

Complex	S	Complex number
$[Fe^{III}(py)(L_{S,S})_2]^-$	3/2	**1**
$[Fe^{III}(py)(L_{S,S})_2]^-$	3/2	**2**
$[Fe^{III}(py)(L^{\bullet}_{S,S})(L_{S,S})]^0$	1	**3**
$[Fe^{III}(py)(^1L^{\bullet}_{S,S})(L_{S,S})]^0$	1	**4**
$[Fe^{III}(Me\text{-}py)(L^{\bullet}_{N,N})(L_{N,N})]^0$	1	**5**
$[Fe^{III}I(L^{\bullet}_{TSC})_2]^0$	1	**6**
$[Fe^{III}I(^1L^{\bullet}_{S,S})_2]^0$	1/2	**7**
$[Fe^{III}(CN)(^2L^{\bullet}_{S,S})_2]^0$	1/2	**8**
$[Fe^{III}I(^3L^{\bullet}_{N,S})_2]^0$	1/2	**9**
$[Fe^{III}I(L^{\bullet}_{N,N})_2]^0$	1/2	**10**
$[Fe^{III}Cl(^4L^{\bullet}_{N,N})_2]^0$	1/2	**11**
$[Fe^{II}(CN)(^2L^{\bullet}_{S,S})_2]^-$	0	**12**
$[Fe^{II}(CN\text{-}Me)(L^{\bullet}_{N,N})_2]^0$	0	**13**
$[Fe^{III}(CN)_2(L^{\bullet}_{TSC})_2]^-$	0	**14**

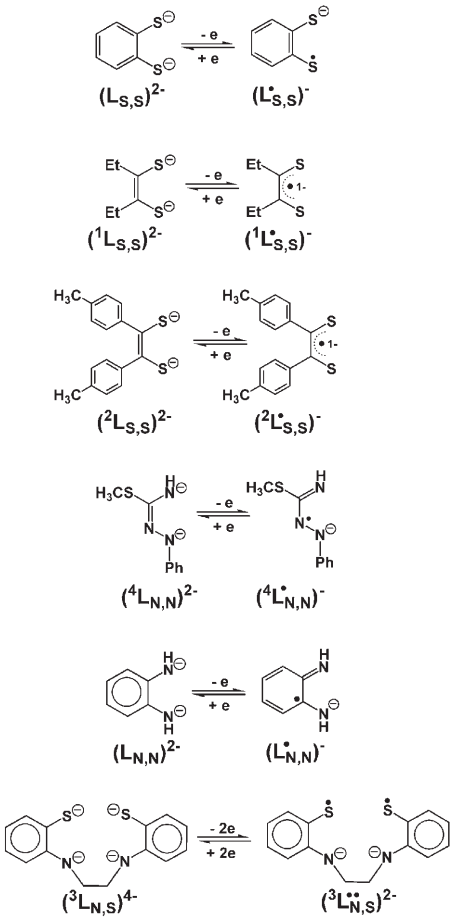

Scheme 1.

Results and Discussion

Complexes with zero π-radical ligands: To calibrate the DFT methodology used here we have first investigated two

structurally and spectroscopically well-characterized complexes of iron(III), namely **1**[9] and **2**,[10] both of which contain two *S*,*S*′-coordinated, closed-shell dianions (benzene-1,2-dithiolate(2−) in **1** and 1,2-diethyl-en-1,2-dithiolate(2−) in **2** and a fifth apical pyridine ligand: $[Fe^{III}(py)(S_2C_6H_4)_2]^-$ (**1**) and $[Fe^{III}(py)(S_2C_2Et_2)_2]^-$ (**2**). These monoanions possess a square-based pyramidal FeS_4N polyhedron with a central, intermediate-spin ferric ion ($S_{Fe}=S_t=3/2$; $\mu_{eff}=3.87\ \mu_B$).

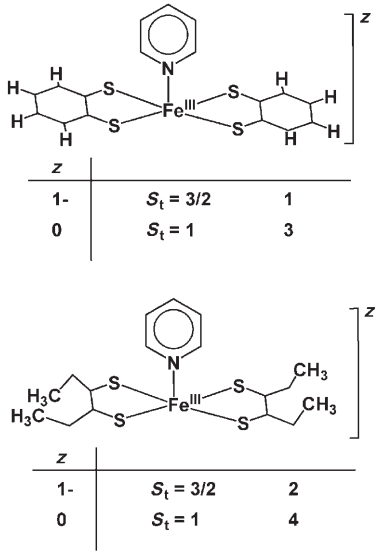

Simple ligand-field theoretical considerations predict an electronic structure in which three unpaired electrons reside in three metal-d based molecular orbitals (MOs). Complexes **1**[9] and **2**[10] have been characterized by X-ray crystallography. The Mössbauer spectral parameters have been reported for **1**[9] only (Table 2).

The geometries of **1** and **2** were optimized by using the B3LYP hybrid functional for an spin-unrestricted $M_S \approx S = 3/2$ system. The results are summarized in Table 3. The

Table 2. Spin states and Mössbauer parameters of complexes.

			Experimental values			Calculated values	
	S_t[a]	S_{Fe}[b]	δ[c] [mm s^{-1}]	ΔE_Q[d] [mm s^{-1}]	Ref.	δ[c] [mm s^{-1}]	ΔE_Q[d] [mm s^{-1}]
1	3/2	3/2	0.33	3.03	[9]	0.39	3.43
2	3/2	3/2	n.m.[e]	n.m.	[10]	0.40	3.27
3	1	3/2	0.29	3.02	[9]	0.34	3.17
4	1	3/2	n.m.	n.m.	[10]	0.34	2.96
5	1	3/2	0.20[f]	3.06	[14]	0.18	2.90
6	1	3/2	0.17	2.96	[20,21]	0.07	2.63
7	1/2	3/2	n.m.	n.m.	[10]	0.29	2.61
8	1/2	3/2	0.25	1.93	[15]	0.17	2.05
9	1/2	3/2	0.11[f]	3.41	[16]	0.16	3.05
10	1/2	3/2	0.15[f]	3.03	[14]	0.14	2.59
11	1/2	3/2	0.20	2.21	[17]	0.20	2.21
12	0	0	0.11	2.59	[15]	0.16	2.62
13	0	0	0.09	2.60	[15]	0.06	2.62
14	0	1/2	0.08[f]	1.01	[21]	0.12	1.53

[a] Ground state of molecule. [b] Intrinsic spin state of central iron ion. [c] Isomer shift at 80 K vs. α-Fe at 298 K. [d] quadrupole splitting at 80 K. [e] n.m. = not measured. [f] 4.2 K.

Table 3. Experimental and calculated bond lengths [Å] of complexes **1**–**4**, **7**.

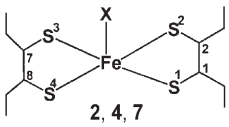

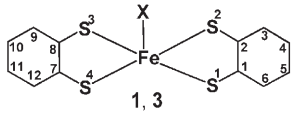

	2		**4**	**7**		**1**		**3**
	Exptl[a]	Calcd	Calcd	Exptl[b]	Calcd	Exptl[c]	Calcd	Calcd
Fe–X	2.172	2.303	2.247	2.558	2.618	2.155	2.298	2.237
Fe–S1	2.230	2.286	2.256	2.187	2.258	2.234	2.289	2.267
Fe–S2	2.231	2.286	2.255	2.178	2.264	2.235	2.288	2.267
Fe–S3	2.222	2.287	2.261	2.181	2.263	2.253	2.287	2.268
Fe–S4	2.225	2.287	2.264	2.185	2.259	2.226	2.289	2.268
S2–C2	1.768	1.786	1.753	1.701	1.720	1.765	1.776	1.753
C1–C2	1.341	1.360	1.379	1.376	1.395	1.404	1.416	1.423
C1–S1	1.766	1.786	1.753	1.699	1.719	1.760	1.776	1.753
C8–S3	1.751	1.785	1.745	1.696	1.720	1.771	1.776	1.753
C7–C8	1.338	1.359	1.382	1.387	1.395	1.401	1.416	1.423
C7–S4	1.761	1.785	1.746	1.701	1.720	1.755	1.776	1.753
C2–C3						1.402	1.408	1.414
C3–C4						1.388	1.400	1.388
C4–C5						1.394	1.404	1.411

[a] Reference [10]. [b] Reference [10]. [c] Reference [9].

agreement between the experimental and calculated C–S, C–C, and C–N bond lengths is excellent in both cases. Clearly, both ligands in each structure are closed-shell dithiolate(2−) dianions; the average C–S bond length at 1.78 Å is long and indicates single-bond character. The average C–C bonds at 1.40 Å in **1** is typical for an aromatic benzene ring. Similarly, in **2** the ligands are also closed-shell dithiolate dianions. The experimental and calculated data for the neutral pyridine rings are also in excellent agreement. In contrast, the calculated Fe–X bonds are ≈0.06–0.09 Å longer than the corresponding experimental ones. This overestimation is typical for the B3LYP functional.

The molecular orbital (MO) scheme for **1** is shown in Figure 1. A doubly-occupied metal-d orbital and three singly-occupied, metal-based d-orbitals (SOMO's) have been identified. In addition, an empty, predominantly metal-based d-orbital has been found as the lowest unoccupied MO (LUMO). This σ-antibonding d-orbital is energetically well separated from the other four d-orbitals. These are exactly the features of an intermediate-spin ferric ion ($S_{Fe}=3/2$) as predicted by simple ligand-field theory. This notion is further confirmed by the Mulliken spin-population analysis shown in Figure 1 (bottom). It is evident that the spin density is almost exclusively localized on the central iron ion (2.9 unpaired electrons), the pyridine nitrogen atom carries 0.015 unpaired spins. Most significantly, there is no spin density located on the two benzene-1,2-dithiolate(2−) ligands. A closely analogous analysis applies to **2** (see Supporting Information). Again the two 1,2-dithiolato(2−) ligands carry no significant spin density and the three unpaired electrons reside in three metal d-based MOs.

Within the present B3LYP DFT framework it is possible to calculate[8] Mössbauer parameters, namely the isomer shift (δ) and the quadrupole splitting (ΔE_Q) of the central

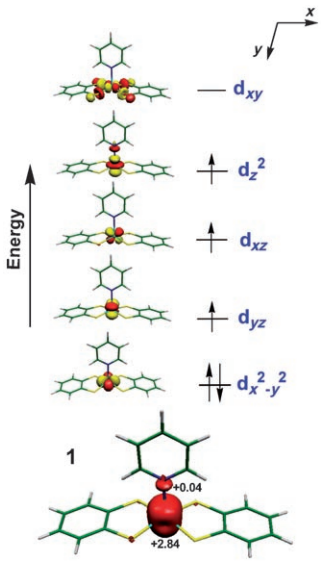

Figure 1. Qualitative MO scheme for the monoanion in complex **1** as derived from a DFT (B3LYP) calculation ($S=3/2$) (top) and spin density plot together with a value of the spin density of the Mulliken spin population analysis (bottom).

iron ion. The calculated values of δ and ΔE_Q for **1** are at 0.39 mm s^{-1} and 3.43 mm s^{-1}, respectively, which are in excellent agreement with the experimental data at 80 K: $\delta=$ 0.33 mm s^{-1} and $\Delta E_Q=3.03$ mm s^{-1}. Note that both, the Mössbauer isomer shift and the quadrupole splitting parameters are sensitive reporters of the POS as well as the intrinsic spin state of the iron ion. Hence, the excellent agreement between theory and experiment confirms the theoretical oxidation state assignment for **1**. For **2** no experimental data exist, but based on the calculations they should be similar to those of **1**. However, for the closely related complex **A** $\delta=$ 0.36 mm s^{-1} and $|\Delta E_Q|=2.64$ mm s^{-1} were reported at 77 K;[11] these values are in good agreement with the calculations for **2**.

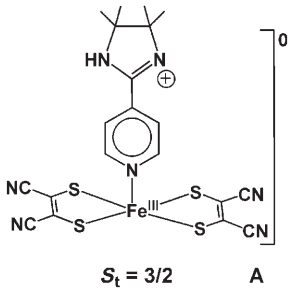

This comparison underlines the reliability of the present DFT approach for the prediction of the geometrical and spectroscopic parameters in five-coordinate iron complexes with an (intrinsic) intermediate spin ($S_{Fe}=3/2$) and closed-shell ligands.

Complexes containing one π-radical ligand: Complexes **1** and **2** can undergo electrochemical or chemical one-electron oxidation,[9,10] generating the paramagnetic ($S_t=1$), neutral complexes $[Fe(py)(S_2C_6H_4)_2]^0$ (**3**) and $[Fe(py)(S_2C_2Et_2)_2]^0$ (**4**), the electronic structures of which have been a matter of debate, since their original phosphine containing analogues $[Fe(PR_3)(S_2C_6H_4)_2]^0$ have been described as iron(IV) species[12] ($S_{Fe}=S_t=1$, d^4) with two closed-shell dithiolate(2−) ligands and a closed-shell, neutral phosphine. By contrast, the spectroscopic data have shown that a description as $[Fe^{III}(py)(S_2C_6H_4^{\bullet})(S_2C_6H_4)]$ with an intermediate-spin ferric ion ($S_{Fe}=3/2$) coupled antiferromagnetically to a delocalized π-radical ligand ($S_{rad}=1/2$) yielding the observed $S_t=1$ ground state is appropriate.[9]

Starting from the optimized geometries of the monoanions **1** and **2**, the geometries of neutral **3** and **4** were relaxed using the BS(3,1) B3LYP method. The results are given in the supporting information and Table 3. Alternatively, we have also pursued a standard spin-unrestricted $M_S=1$ calculation; however, this converged to the same result as the BS-(3,1) calculation. The corresponding high-spin state (BS(4,0) or $M_S=2$) was found to be 8 kcal mol^{-1} higher in energy.

The overall geometries of the two monoanions (**1** and **2**) and of the two neutral complexes (**3** and **4**) are very similar. The most distinct differences are that the average C–S distances in **1** and **2** decrease slightly by 0.02 and 0.035 Å on going to **3** and **4**, respectively. The calculated average Fe–S distances in **1** and **2** are at 2.288 and 2.287 Å, respectively. They also decrease slightly to 2.267 Å in **3** and 2.257 Å in **4**. It is not possible to unambiguously derive an oxidation state of the iron ion in **3** and **4** or to determine safely an oxidation level of the ligands from such minor variations in the calculated geometries or from the similarly minor variations observed experimentally for the phosphine analogues.[9,12]

Figure 2 exhibits a qualitative MO scheme for **3** from the corresponding orbital analysis.[5] We have identified one doubly-occupied, metal-based d orbital, three α-spin SOMO's (metal-centered), and one empty d orbital (LUMO). Interestingly, one of the three SOMOs interacts with a half-filled ligand π orbital (β-spin). The interaction is strongly antiferromagnetic with a spatial overlap of $S_{ab}=$ 0.61, which is a signature of a spin-singlet-coupled electron pair. An estimate of the exchange coupling constant J according to the Yamaguchi approach reference [13] in Equation (1), based on $\hat{H}_{HDvV}=-2J\hat{S}_A\hat{S}_B$, yielded a value of −830 cm^{-1} for **3**.

$$J=-\frac{E_{HS}-E_{BS}}{\langle S^2\rangle_{HS}-\langle S^2\rangle_{BS}} \quad (1)$$

The MO scheme for **4** is very similar and not shown (see Supporting Information).

The Mulliken spin population analysis (shown at the bottom of Figure 2) supports the view that the electronic structure of **3** should be described as intermediate-spin ferric with 2.8 α-spin at the iron(III) ion and 0.86 β-spin distributed over both dithiolene ligands. Similarly, for **4** we find

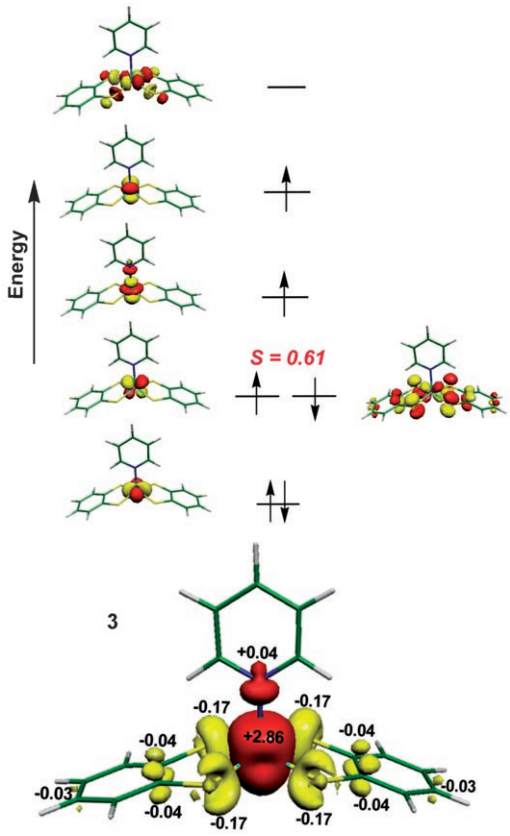

Figure 2. Qualitative MO scheme of the corresponding orbitals of magnetic pairs of **3** as derived from BS(3,1) DFT calculation (top) and spin density plot together with values of the spin density of the Mulliken spin population analysis.

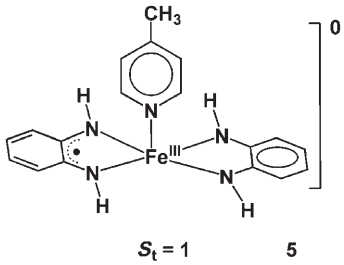

shown in the Supporting Information together with the optimized structural data that are in excellent agreement with experiment.[14] The analysis of the electronic structure according to the protocol described above reveals that complex **5** also contains an intermediate-spin ferric ion ($S_{Fe}=3/2$; d^5) and a delocalized $[Fe^{III}(L^{\bullet}_{N,N})(L_{N,N})]\leftrightarrow[Fe^{III}(L_{N,N})(L^{\bullet}_{N,N})]$ unit that is antiferromagnetically coupled to an $S_t=1$ ground state [$J=-1063\ cm^{-1}$ according to Eq. (1)]. The spin density plot is shown in Figure 3. According to the Mulliken

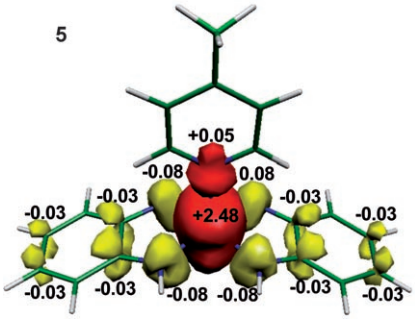

Figure 3. Spin density plot of neutral **5** (the indicated values were derived from a Mulliken spin population analysis of the BS(3,1) B3LYP solution).

2.8 α-spin at the ferric ion and 0.8 β-spin distributed over both dithiolenes. In **3** and **4** we are thus dealing with a case of ligand mixed valency (dithiolate(2−)/dithiolate(1−) π radical) of class III. Experimentally, this description is supported by the observation of an intense ($0.7\times10^4\ M^{-1}cm^{-1}$) intervalence charge-transfer band (IVCT) at 814 nm in the electronic spectrum of **3** that is absent in the spectra of **1** and **2**. The optical absorption spectrum of **4** has not been reported.

It is gratifying to observe that the calculated Mössbauer parameters for **3** agree nicely with the experimental data reference [9] (Table 2). This corroborates the correctness of our electronic structure description of **3** and **4**. The fact that complexes **1**–**4** contain an intermediate-spin ferric ion ($S_{Fe}=3/2$) is also nicely confirmed by the observation that **1** and **3** display similar experimental and calculated Mössbauer parameters irrespective of their differing ground states ($S_t=3/2$ for **1**; but $S_t=1$ for **3**). A metal-based oxidation can therefore safely be ruled out.

The neutral phenylenediamine derivative [Fe(Me-py)-$(L_{N,N})_2$] (**5**) with an $S_t=1$ ground state[14] has a similar molecular and electronic structure as the above sulfur-containing complexes **3** and **4**. The MO scheme obtained from a BS-(3,1) DFT calculation closely resembles that of **3** and is analysis there are 2.4 α-spins at the iron center and 0.44 β-spins distributed over both $(L_{N,N})^n$ ligands. The calculated and experimental Mössbauer data (Table 2) are in excellent agreement with experiment.

Complexes containing two π-radical ligands: Complexes **7**–**11** (Table 1) are neutral species with an $S=1/2$ ground state; they are five-coordinate with two bidentate π-radical, monoanions in the basal plane and a monoanionic chloride, iodide or cyanide ligand in the fifth apical position of a square-based pyramide. With the exception of **8** the structures of all species have been determined by X-ray crystallography.

Complex **7**[10] contains two π-radical monoanions derived from 1,2-diethylene-1,2-dithiolate(2−), $(^1L^{\bullet}_{S,S})^-$; complex **8**[15] has two such radicals derived from 1,2-di-*p*-tolyl-1,2-enedithiolate(2−); complex **9**[16] contains two *o*-aminothiophenolate-derived π radicals bridged by an ethane group; complex **10**[14] contains two *o*-phenylenediamide(2−)-derived monoanionic π radicals; and complex **11**[17] has two π-radical mon-

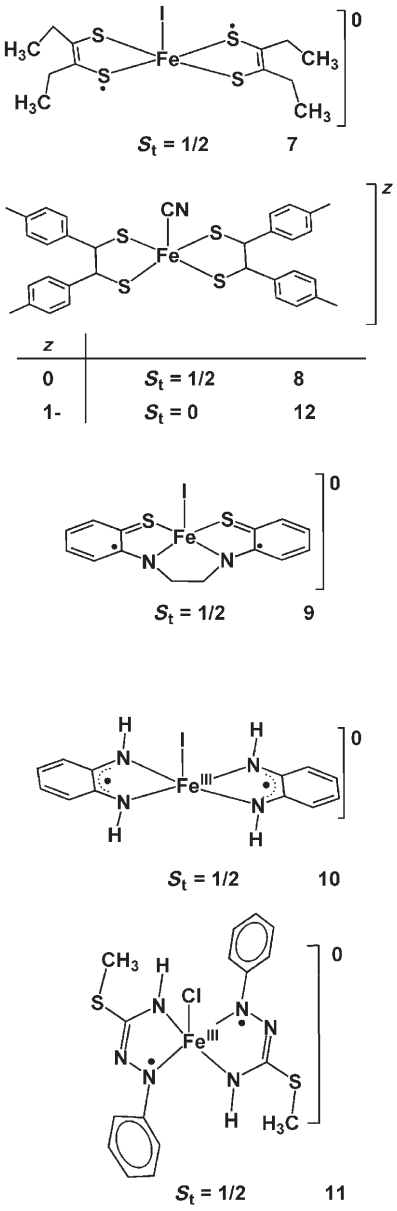

oanions derived from *S*-methyl-1-phenyl-isothiosemicarbazide(2−).

As is clearly deduced from the data in Table 2 the Mössbauer parameters of complexes **8**–**11** are quite similar: the isomer shifts span a narrow range of 0.29–0.14 mm s^{-1}, whereas the quadrupole splittings are in the range 2.05–3.05 mm s^{-1}. This is a clear indication that their electronic structures are very similar: in each case two π-radical monoanions ($S_{rad}=1/2$) are antiferromagnetically coupled to an intermediate-spin, central ferric ion ($S_{Fe}=3/2$) yielding the observed $S_t=1/2$ ground state. A BS(3,2) DFT calculation with the B3LYP functional has been reported for **8** in reference [15] and corroborates the above notion: one doubly-occupied metal-based d orbital, three metal-based SOMOs, and an unoccupied Fe d orbital have been identified (intermediate-spin Fe^{III}). Two of these metal SOMOs are antiferromagnetically coupled to two half-filled ligand-based orbitals through π pathways. The spatial overlap of the corresponding orbitals is strong ($S_{ab}=0.77$ and 0.57, respectively). The exchange coupling constant is calculated to be $J=-1419$ cm^{-1}. The calculated Mössbauer parameters, again, agree nicely with the experimental data (Table 2). We note that in these calculations a truncated model was employed in which the *p-tert*-butyl groups have been replaced by methyl groups.

As pointed out above, the structure of **8** has not been determined. Therefore, we have carried out calculations on the very similar complex $[Fe^{III}I(^1L^{\bullet}_{S,S})_2]^0$ (**7**) for which the structure has been reported[10] (Table 3). The agreement of the calculated data from the BS(3,2) solution and the experimental data is very good. Note that the average C–S bond lengths at 1.70 (exptl) and 1.72 Å (calcd) are in excellent agreement; they are much shorter than those in **2** at 1.76 (exptl) and 1.786 Å (calcd), which indicates that the ligands in **2** are closed-shell dianions $(^1L_{S,S})^{2-}$, while they are best described as paramagnetic π-radical monoanions $(^1L^{\bullet}_{S,S})^{-}$ in **7**. Similarly, the "olefinic" C–C bonds of the ligands in **7** are long at 1.38 (exptl) and 1.395 Å (calcd), but significantly shorter at 1.34 (exptl) and 1.36 Å (calcd.) in **2** as is expected for $(^1L^{\bullet}_{S,S})^{-}$ and $(^1L_{S,S})^{2-}$, respectively. These values are intermediate in **4** containing one radical and one closed-shell dianion.

Figure 4 displays the qualitative MO scheme for **7** together with the spin density plot. The former agrees nicely with that reported for **8**:[15] an intermediate-spin ferric ion ($S_{Fe}=3/2$) is antiferromagnetically coupled to two $(^1L^{\bullet}_{S,S})^{-}$ π radicals. The Mulliken analysis indicates 2.6 α-spins at the iron

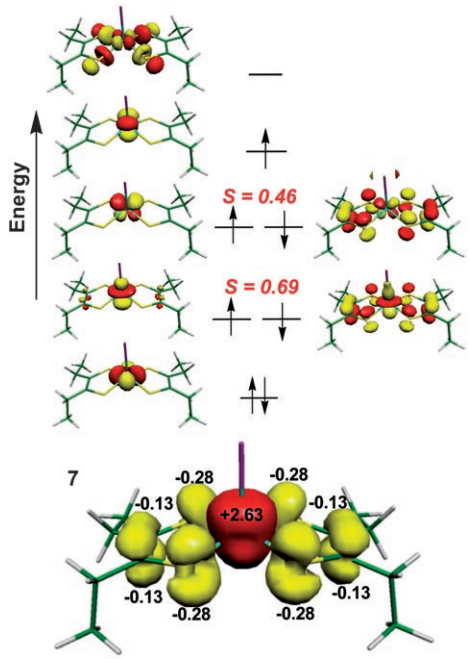

Figure 4. Qualitative MO scheme for neutral **7** as derived from a BS(3,2) DFT calculation (B3LYP) (top) and a spin density plot (bottom) from a Mulliken spin population analysis.

ion and 0.8 β-spins on each bidentate ligand. About 65% of the ligand spin population resides on the sulfur atoms and only ≈30% is distributed over the two olefinic C–C atoms of each ligand. This result implies that in **7** there are two essentially sulfur-centered π-radical monoanions $(^1L^{\bullet}_{S,S})^-$ present: $[Fe^{III}I(^1L^{\bullet}_{S,S})_2]^0$ ($S_t=1/2$). Hence, the electronic structure cannot be described as $[Fe^{V}I(^1L_{S,S})_2]$.

It is instructive to compare the spin densities in **2** (($S=3/2$), **4** ($S=1$), and **7** ($S=1/2$): there is essentially no spin density on both noninnocent dithiolene ligands in **2**; one unpaired electron is distributed over two such ligands in **4**, and one unpaired electron is located on each $(^1L^{\bullet}_{S,S})^-$ π-radical ligand in **7**; the ferric ions possess invariably ≈3 unpaired electrons (intermediate spin ($S_{Fe}=3/2$)).

Sellmann's complex **9**[16] contains two *N*,*S*-coordinated o-aminobenzenethiolate-derived ligands that are bridged by an -CH_2–CH_2- group. The optimized BS(3,2) B3LYP/TZVP geometry (including the ZORA relativistic correction for iodine) agrees nicely with the experimental crystal structure (Table 4). The qualitative MO scheme in Figure 5 clearly shows that an intermediate-spin ferric ion is antiferromagnetically coupled to two π radicals in $(^3L^{\bullet\bullet}_{N,S})^{2-}$. The spin density plot of **9** shown in Figure 5 (bottom) reveals α-spin population (2.4 e^-) at the iron ion and 0.6 β-spins on each π radical part of the ligand. The calculated Mössbauer parameters agree very well with the reported experimental data (Table 2). We note that the present calculations (and the experimental spectroscopic results[16]) rule out the previously proposed description of the electronic structure of **9** as Fe^V (d^3) with a closed-shell tetraanion $(^3L_{N,S})^{4-}$ (Scheme 1).[16]

Table 4. Experimental and calculated bond lengths [Å] of complexes **9** and **10**.

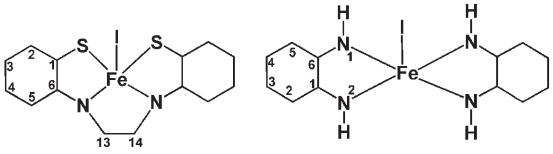

9 **10**

	9			**10**	
	Exptl[a]	Calcd		Exptl[b]	Calcd
Fe–I	2.555	2.623	Fe–I	2.598	2.661
Fe–N	1.846	1.890	Fe–N	1.890(av.)	1.905
Fe–S	2.184	2.251			
C13–C14	1.506	1.537			
N–C6	1.340	1.347	N–C	1.345(av.)	1.339
N–C14	1.458	1.461	C1–C6	1.436	1.447
S–C1	1.718	1.732	C1–C2	1.418	1.419
C1–C6	1.416	1.439	C2–C3	1.370	1.376
C1–C2	1.396	1.409	C3–C4	1.419	1.424
C2–C3	1.370	1.380	C4–C5	1.377	1.376
C3–C4	1.402	1.416	C5–C6	1.418	1.419
C4–C5	1.357	1.376			
C5–C6	1.411	1.422			

[a] Reference [16]. [b] Reference [14].

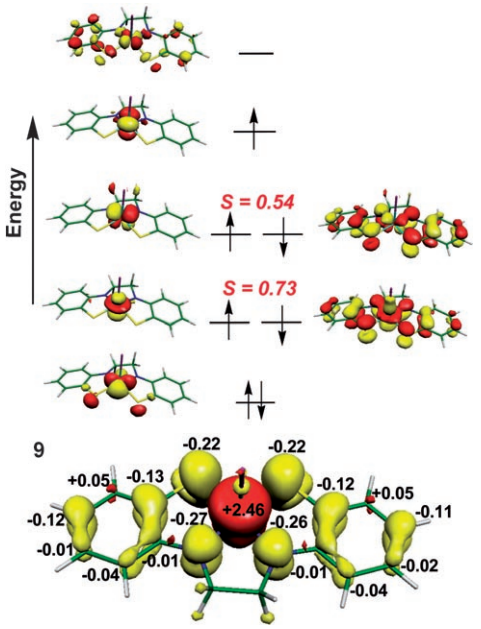

Figure 5. Qualitative MO scheme for neutral **9** as derived from a BS(3,2) DFT calculation (B3LYP/ZORA) (top) and a spin density plot (bottom) from a Mulliken spin population analysis.

The structural and spectroscopic data of **10**[14] are also very well reproduced by the BS(3,2) B3LYP/TZVP/ZORA calculations (Table 4). The qualitative MO scheme and the spin density plot displayed in Figure 6 show that its electronic structure is the same as in **7**, **8**, and **9**: an intermediate-spin ferric ion is antiferromagnetically coupled to two π radicals $(L^{\bullet}_{N,N})^-$.

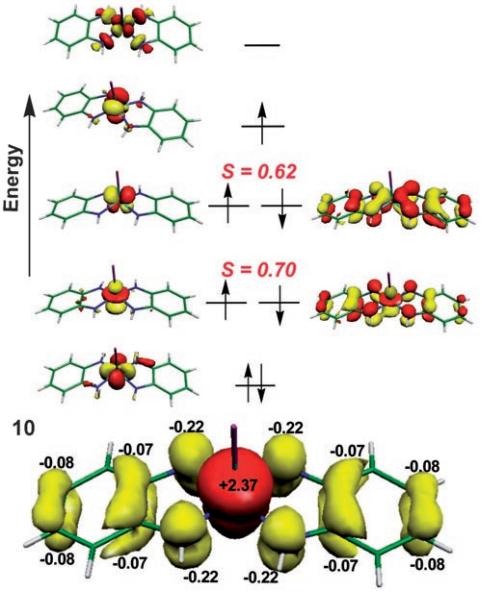

Figure 6. Qualitative MO scheme for neutral **10** as derived from a BS(3,2) DFT calculation (B3LYP/ZORA) (top) and a spin density plot (bottom).

The *S*-methyl-1-phenyl-isothiosemicarbazide π-radical monoanion, $(^4L^{\bullet}_{N,N})^-$, has been identified in a number of complexes of which the diamagnetic square planar complex $[Ni^{II}(^4L^{\bullet}_{N,N})_2]$ is probably the most characteristic.[18] In principle, this ligand can exist in its one-electron oxidized form, namely neutral $(^4L_{N,N}{}^{Ox})^0$, and a two-electron reduced form $(^4L_{N,N}{}^{red})^{2-}$. The former has been identified in octahedral paramagnetic *trans*-$[Ni^{II}(^4L_{N,N}{}^{Ox})_2I_2]$;[19] the reduced dianion has to our knowledge not been characterized in a coordination compound (Figure 7).

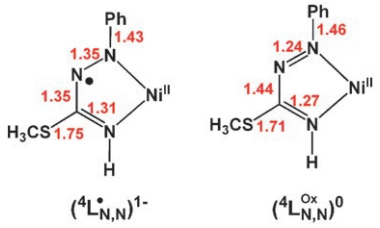

Figure 7. Experimental bond lengths (Å) of *N*,*N*-coordinated $(^4L^{\bullet}_{N,N})^-$ in $[Ni^{II}(^4L^{\bullet}_{N,N})_2]$ from reference [18] and of $(^4L_{N,N}{}^{Ox})^0$ in *trans*-$[Ni^{II}(^4L_{N,N}{}^{Ox})_2I_2]$ from reference [19].

The paramagnetic iron complex **11** ($S=1/2$) has been synthesized and structurally characterized.[17] The geometry of the ligand resembles closely that in the nickel complex $[Ni^{II}(^4L^{\bullet}_{N,N})_2]$ and, therefore, an electronic structure containing two π-radical ligands antiferromagnetically coupled to a central intermediate-spin ferric ion has been proposed.

BS(3,2) B3LYP calculations of **11** are in agreement with this proposal. Table 5 demonstrates excellent agreement between calculated and experimental bond lengths in **11**. It is also gratifying to observe that the experimental and calculated Mössbauer parameters are in good agreement.

Table 5. Comparison of experimental and calculated bond lengths [Å] in complex **11**.

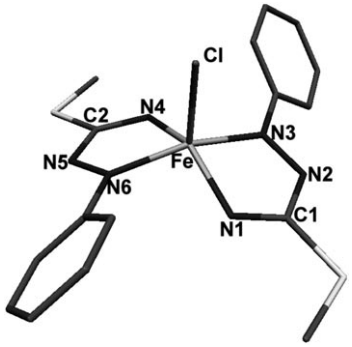

	Exptl[a]	Calcd		Exptl[a]	Calcd
Fe–Cl	2.2863(6)	2.291	N1–C1	1.313(3)	1.318
Fe–N1	1.889(2)	1.930	C1–N2	1.352(3)	1.346
Fe–N3	1.892(2)	1.935	N2–N3	1.339(3)	1.325
Fe–N4	1.892(2)	1.930	N4–C2	1.307(3)	1.318
Fe–N6	1.882(2)	1.936	C2–N5	1.350(3)	1.345
			N5–N6	1.335(3)	1.325

[a] Data from reference [17].

Figure 8 shows the spin density plot. Clearly, an intermediate-spin ferric ion (2.5 unpaired e^-) is present (α-spin) and two π-radical ligands (two β-spins of each −0.70).

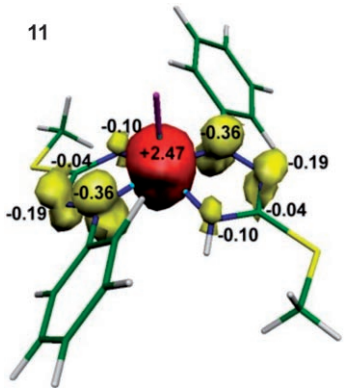

Figure 8. Spin density plot of neutral **11**.

Complexes 12 and 13: The monoanionic complex **12** possesses an $S_t=0$ ground state. The molecular and electronic structure of this species has been calculated by DFT (B3LYP) in reference [15]. Three doubly-occupied metal-based d orbitals have been identified which is characteristic of a low-spin ferrous ion ($S_{Fe}=0$). The HOMO and LUMO are 83 and 70% ligand in character, respectively. In addition, two empty metal-based d orbitals above the LUMO have been found. Thus, an electronic structure of **12** as in $[Fe^{II}(CN)(^2L^{\bullet}_{S,S})_2]^-$ ($S_t=0$; $S_{Fe}=0$) in which the two π radicals are strongly antiferromagnetically coupled is the most appropriate description. Note that experimental and calculated Mössbauer parameters agree nicely (Table 2).

One-electron oxidation of monoanionic **12** yields neutral **8** which has in a similar fashion been characterized (see above) as $[Fe^{III}(CN)(^2L^{\bullet}_{S,S})_2]^0$ containing an intermediate-spin ferric ion ($S_{Fe}=3/2$), which is antiferromagnetically coupled to two π radicals $(^2L^{\bullet}_{S,S})^-$ yielding an $S_t=1/2$ ground state (see above). Thus, the redox reaction **12**→**8**+e^- is a metal-centered process.

It is now very interesting to investigate the electronic structure of the diamagnetic nitrile complex **13** using the BS DFT methodology. On the basis of its experimental data,[14] two differing electronic structures are conceivable for **13**: $[Fe^{II}(CNMe)(L^{\bullet}_{N,N})_2]^0$ containing a low-spin ferrous ion (d^6, $S_{Fe}=0$) and two antiferromagnetically coupled π-radical ligands or an intermediate-spin ferrous ion (d^6, $S_{Fe}=1$) coupled antiferromagnetically to two π-radical ligands $(L^{\bullet}_{N,N})^-$.

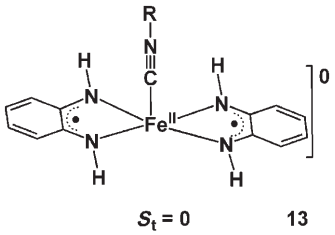

$S_t = 0$ 13

Therefore, three BS DFT (B3LYP) calculations were carried out without imposing any constraints: 1) closed-shell $S=M_S=0$, 2) BS(1,1) (invoking two ligand radicals), and 3) BS(2,2). The latter two calculations converged to the same BS(0,0) (closed-shell) solution with identical geometry and Mössbauer data. We have also calculated a closed-shell solution ($S=0$) using the BP86 functional. For all these calculations the agreement between the experimental and calculated Mössbauer parameters is poor. Inspection of the optimized geometries reveals that the bond lengths in the $[Fe^{II}(L^{\bullet}_{N,N})_2]$ unit are always satisfactorily reproduced in comparison with the experimental data (Supporting Information). The Fe–C bond was calculated to be significantly shorter in all models than the experimental value ($\Delta=0.07$ Å). This is unusual, since it is commonly observed that metal–ligand distances are overestimated by 0.05–0.10 Å with the present methodology. Thus, in the present case the π-acceptor properties of the methylnitrile ligand are grossly overestimated in the calculations. We have therefore introduced one constraint and fixed the Fe–C value at 1.840 Å, which is the experimental distance. Following this modification the calculated Mössbauer isomer shift value agrees beautifully with experiment (as does the optimized structure). Interestingly, both BP86 closed-shell solutions (with and without the constraint) are nearly isoenergetic. The short $C-N_{imino}$ bonds and the quinoid-type distortions of the two six-membered basal rings point to the presence of two *o*-diiminobenzosemiquinonate(1−) π radicals.

Qualitative MO diagrams for **13** derived from the BP86 DFT calculations with (top) and without (bottom) the above constraint are shown in Figure 9. Both computed electronic structures are basically derived from a low-spin ferrous ion, since three doubly occupied and two virtual metal-based d orbitals are identified. However, the constraint-free model displays a HOMO with 56% metal d character in contrast to the more realistic constrained model

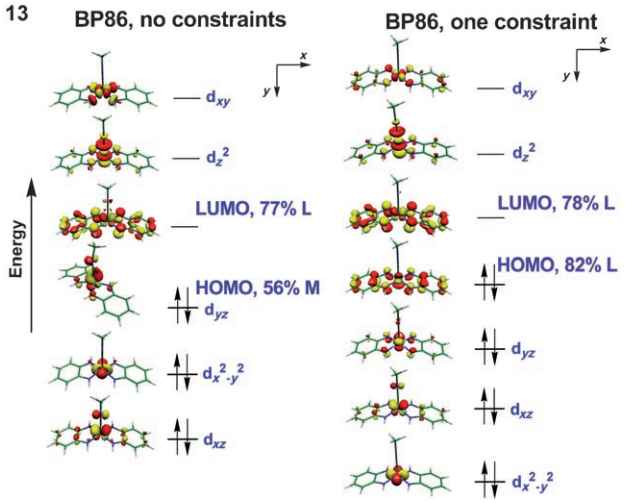

Figure 9. Kohn-Sham MOs for $[Fe^{II}(L^{\bullet}_{N,N})_2(CN\text{-}Me)]$ (**13**) as obtained from unconstrained, restricted (left) and constrained, restricted (right) BP86 calculations.

for which the HOMO is essentially diimine ligand-centered (82%). Thus, the underestimation of the Fe–CNMe bond length results in an unrealistically strong covalent interaction through π backbonding. This is not in agreement with experiment. For instance, the C≡N stretching frequency in **13** is observed at 2113 cm^{-1}, which is very close to the value observed for the free ligand (2132 cm^{-1}). This observation clearly argues against strong π backbonding in **13**.

This effect is also nicely borne out by the calculated isomer shift parameter. For the constrained model the isomer shift parameter is calculated at 0.06 $mm\,s^{-1}$ in close agreement with experiment (0.09 $mm\,s^{-1}$), while for the unconstrained model $\delta=-0.02$ $mm\,s^{-1}$. Hence, in **13** we meet one of the relatively rare cases in which the BS DFT methodology is not fully satisfactory. This shortcoming is immediately detected by comparing experimental and calculated spectroscopic parameters. Hence, the importance of seeking as close feedback from experiment in deriving electronic structures from theoretical calculations can hardly be overemphasized.

Complexes containing pentane-2,4-dione-bis(*S*-alkylisothiosemicarbazonato)^n ligands ($n=3-$, $2-$, $1-$): Gerbeleu et al.[20] and Wieghardt et al.[21] have reported five-coordinate iron complexes containing a basal, tetradentate pentane-2,4-dione-bis(*S*-alkylisothiosemicarbazide) ligand and an apical iodide. The spectroscopic data (UV/Vis and Mössbauer spectra) and the paramagnetic ground state $S=1$ of complex **6**[21] and its *S*-ethyl derivative[20] are apparently in accord with an electronic structure in which the central iron ion possesses a +IV POS (d^4; $S_{Fe}=1$) and a diamagnetic, trianionic isothiosemicarbazide(3−) (Scheme 2) and an iodide ligand: $[Fe^{IV}(L^{Red}_{TSC})I]$ (**6**).

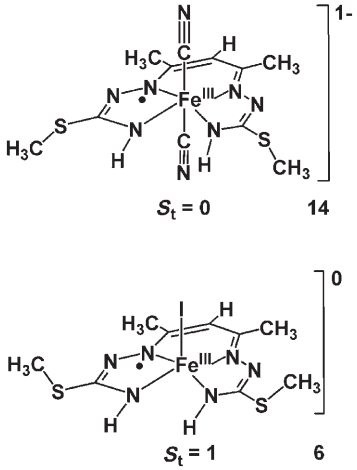

It has also been proposed that in diamagnetic, octahedral $[Fe(CN)_2(L^{Ox}_{TSC})]^-$ (**14**) a low-spin Fe^{II} ion (d^6; $S=0$) is present[21] and a monoanionic, diamagnetic ligand $(L^{Ox}_{TSC})^-$ (Scheme 2). Again the reported experimental Mössbauer parameters are apparently in accord with this interpreta-

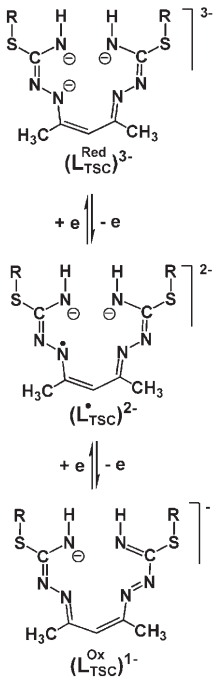

Scheme 2.

tion.[20,21] For both complexes there exist alternative descriptions of their electronic structures if one takes into account the possibility that the ligand can actually be a dianionic π radical, $(L^{\bullet}_{TSC})^{2-}$ ($S_{rad}=1/2$) (Scheme 2).

Complexes **6** and **14** could be formulated as $[Fe^{III}(L^{\bullet}_{TSC})I]$ or $[Fe^{III}(CN)_2(L^{\bullet}_{TSC})]^-$ in which both iron ions possess a +III oxidation state (d^5) of intermediate spin ($S_{Fe}=3/2$) in the former and low spin ($S_{Fe}=1/2$) in the latter. Intramolecular antiferromagnetic coupling would then yield the observed $S_t=1$ ground state in **6** and $S_t=0$ in the six-coordinate monoanion **14**.

To distinguish between these two possibilities we have calculated and optimized the geometries of three hypothetical molecules, namely $[Na^{I}(L^{Ox}_{TSC})]$ ($S=0$); $[Zn^{II}(L^{\bullet}_{TSC})]$ ($S=^1/_2$), and $[Ga^{III}(L^{Red}_{TSC})]$ ($S=0$) by using the B3LYP functional. The results are summarized in Table 6.

It is significant that the C–N, N–N, and C–C distances of the backbone of the 12- $(L^{Ox}_{TSC})^-$, 13- $(L^{\bullet}_{TSC})^{2-}$, or 14-π-electron system $(L^{Red}_{TSC})^{3-}$ do not vary greatly with the oxidation level of the ligand (maximally by 0.03 Å per one-electron change in the N–N bond length and similarly in the two C–NH bonds). Thus, X-ray crystallography of a given complex of this type, even if the structures are of high quality, will not readily allow the experimental identification of the ligand oxidation level.

Table 6. DFT Calculations of the hypothetical molecules $[Na(L^{Ox}_{TSC})]$, $[Zn^{II}(L^{\bullet}_{TSC})]$, and $[Ga^{III}(L^{Red}_{TSC})]$ (B3LYP). Bond lengths are given in Å.

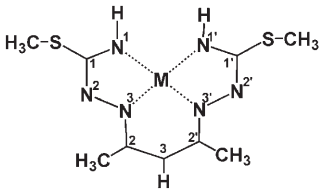

	$[Na^{I}(L^{Ox})]^0$	$[Zn^{II}(L^{\bullet})]$	$[Ga^{III}(L^{Red})]$
M-N1	2.336	1.998	1.927
M-N3	2.402	2.098	1.974
N1–C1	1.307	1.334	1.360
C1–N2	1.396	1.358	1.326
N2–N3	1.326	1.361	1.389
N3–C2	1.358	1.347	1.356
C2–C3	1.419	1.420	1.410
C1–S	1.799	1.786	1.785

Optimization of the geometry of the neutral, five-coordinate **6** with a BS(3,1) $M_S=1$ and a spin-unrestricted $M_S \approx S=1$ model resulted in a single BS solution. The attempted calculation of an $[Fe^{IV}I(L^{Red}_{TSC})]$ electronic structure with an $S_{Fe}=1$ and a diamagnetic ligand $(L^{Red}_{TSC})^{3-}$ converged back to the BS(3,1) $M_S=1$ solution (Table 7).

Table 7. Comparison of experimental and calculated bond lengths [Å] of complexes **6** and **14**.

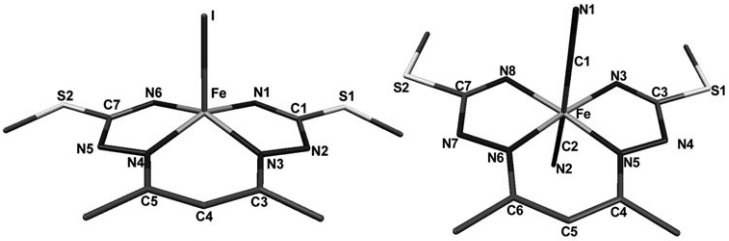

	6			14	
	Exptl[a]	Calcd		Exptl[a]	Calcd
Fe–I	2.593	2.619	Fe–C1	1.955(6)	1.995
Fe–N1	1.857	1.908	Fe–C2	1.947(7)	1.996
Fe–N3	1.883	1.930	Fe–N3	1.969(5)	2.009
Fe–N4	1.890	1.930	Fe–N5	1.874(5)	1.921
Fe–N6	1.864	1.909	Fe–N6	1.839(5)	1.922
N1–C1	1.312	1.333	Fe–N8	1.965(5)	2.009
C1–N2	1.339	1.328	C1–N1	1.154(8)	1.161
N2–N3	1.363	1.358	C2–N2	1.151(9)	1.161
N3–C3	1.365	1.343	N3–C3	1.295(8)	1.301
C3–C4	1.361	1.403	C3–N4	1.330(9)	1.338
C4–C5	1.396	1.403	N4–N5	1.374(7)	1.355
C5–N4	1.369	1.343	N5–C4	1.329(8)	1.337
N4–N5	1.365	1.358	C4–C5	1.396(10)	1.401
N5–C7	1.317	1.328	C5–C6	1.37(1)	1.401
C7–N6	1.316	1.333	C6–N6	1.362(8)	1.337
			N6–N7	1.364(7)	1.355
			N7–C7	1.354(8)	1.338
			C7–N8	1.285(8)	1.301

[a] Data from reference [21].

Figure 10 shows a qualitative MO scheme from which it is clearly established that the central iron possesses a +III oxidation state with intermediate spin $S_{Fe}=3/2$. Thus, the ligand is best described as a π-radical dianion $(L^{\bullet}_{TSC})^{2-}$. Intramolecular antiferromagnetic coupling between one half-filled metal-based d orbital and a half-filled π-radical ligand orbital affords the observed $S_t=1$ ground state. The above calculations allow the conclusion that **6** is not a genuine Fe^{IV} complex with a d^4 ($S_{Fe}=1$) ground state as was claimed in our earlier publication.[21]

The geometry optimization of **14** has been carried out for BS(1,1) $M_S=0$ (Table 7), and a closed-shell $S=0$ state. The BS(1,1) solution was found to be 3.0 kcal mol^{-1} lower in energy than the latter; it is 7.3 kcal mol^{-1} lower than the BS(2,0) $M_S=1$ solution (high spin). The calculated geometry of the ligand $(L^{\bullet}_{TSC})^{2-}$ in $[Zn^{II}(L^{\bullet}_{TSC})]$ is remarkably similar to that calculated here for **14**, and the calculated geometry agrees very well with the experimental one. The Fe–N and

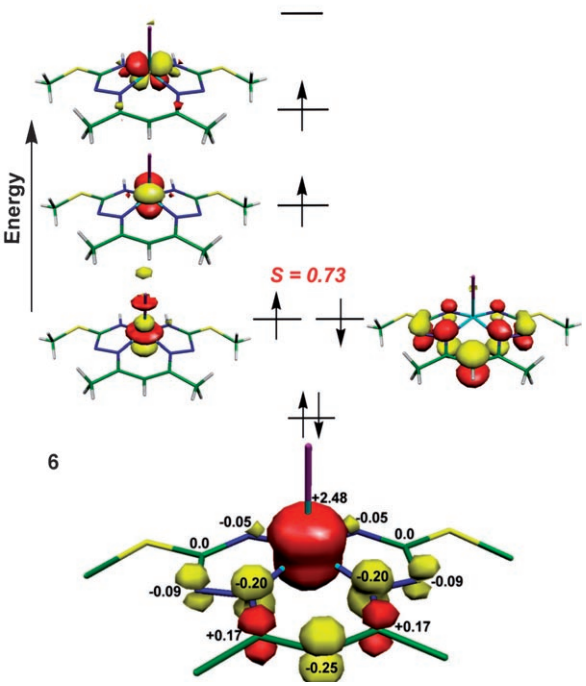

Figure 10. Qualitative MO scheme for **6** as derived from a BS(3,1) DFT calculation (B3LYP) (top) and a spin density plot (bottom) from a Mulliken spin population analysis.

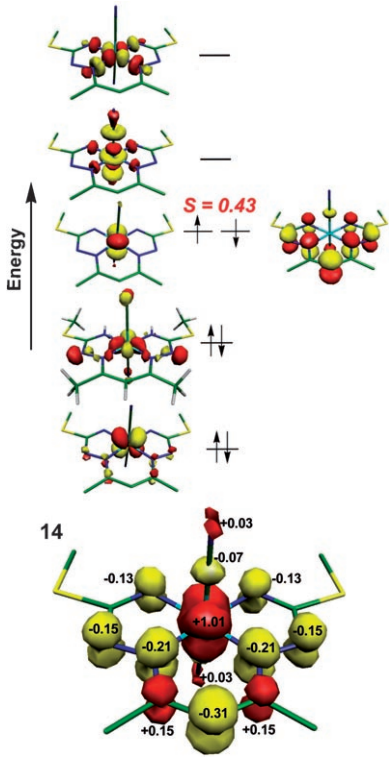

Figure 11. Qualitative MO scheme for **14** as derived from a BS(1,1) DFT calculation (B3LYP) (top) and a spin density plot (bottom) from a Mulliken spin population analysis.

Fe–C bond lengths are overestimated by ≈0.05 Å as is typical for the B3LYP functional.

Figure 11 shows a qualitative MO diagram for **14** (top) and a spin density distribution (bottom). A typical picture for a low-spin ferric ion ($S_{Fe}=1/2$) emerges: two doubly-occupied mainly metal-based d orbitals and a single SOMO of metal d character as well as two empty metal-based d orbitals at higher energies are identified. Interestingly, a singly-occupied ligand orbital is also clearly detected, which couples antiferromagnetically with the metal d SOMO yielding the observed $S_t=0$ ground state ($J=-2200\ cm^{-1}$). The spin density distribution corroborates this picture: one unpaired electron resides at the metal center (α-spin) and one delocalized over the whole ligand $(L^{\bullet}_{TSC})^{2-}$ (β-spin).

Thus, in contrast to the interpretation given in reference [21] the calculations clearly do not support the description of **14** as low-spin ferrous complex containing a diamagnetic $(L^{Ox}_{TSC})^{-}$ ligand; instead, it is best described as $[Fe^{III}(CN)_2(L^{\bullet}_{TSC})]^{-}$. The calculated and experimental Mössbauer parameters for **6** and **14** agree reasonably well.

Conclusions

The most salient results of this study are twofold. First, it is convincingly shown that the electronic structure of compounds containing a paramagnetic transition-metal ion with a d^N configuration and one or two π-radical ligands coupled antiferromagnetically to the metal ion can be safely identified by broken-symmetry density functional calculations. The main problem of identification in the calculations that the solution found corresponds to a spin-coupled metal-radical system rather than to a classical Werner-type coordination compound with closed-shell ligands and a paramagnetic metal ion can be overcome by this methodology. From these electronic structure calculations spectroscopic parameters such as the isomer shift and the quadrupole splitting parameter (and the asymmetry parameter η) of a Mössbauer spectrum can be calculated and compared with the experimental data. Agreement of the data is then taken a solid indication that the calculated electronic structure is indeed the correct one.

Secondly and in particular, in the present series of five-coordinate iron complexes **1**–**14** we have identified the following classes:

1) Complexes **1** and **2** containing an intermediate-spin ferric ion ($S_{Fe}=3/2$) and zero π-radical ligands give rise to an $S_t=3/2$ ground state with three unpaired electrons located in metal d-orbitals. The ligands do not carry significant spin density. This picture is in full agreement with simple ligand field theoretical considerations.
2) Complexes **3**–**6** possess an $S_t=1$ ground state in which an intermediate-spin ferric ion ($S_{Fe}=3/2$) couples antiferromagnetically to a π-radical ligand ($S_{rad}=1/2$). From Mulliken spin population analyses it is possible to show that the central metal ion carries ≈3.0 unpaired electrons (α-spin) and the monoanionic π-radical ligand de-

rived from 1) benzene-1,2-dithiolates, 2) *o*-phenylenediimide, or 3) pentane-2,4-dione-bis-(*S*-alkylisothiosemicarbazonate) carries one electron (β-spin) which in the fist two cases is delocalized over two such ligands (ligand mixed valency of class III). In complex **6** we have identified for the first time the π radical $(L^{\bullet}_{TSC})^{2-}$. In none of the above cases **3**–**6** have the calculations shown evidence for an Fe^{IV} (d^4; $S_{Fe}=1$) configuration in conjunction with closed-shell ligands.

3) Complexes **7**–**11** possess an $S_t=1/2$ ground state in which an intermediate-spin ferric ion ($S_{Fe}=3/2$) couples antiferromagnetically to two π-radical ligands ($S_{rad}=1/2$). The Mulliken spin population analysis clearly show 3 α-spins at the iron ion and two unpaired electrons (β-spins) located on two π-radical ligands. No evidence has been found for Fe^{V} (d^3; $S_{Fe}=1/2$ or 3/2).
4) Complexes **12** and **13** are diamagnetic ($S_t=0$). Both contain a low-spin ferrous ion (d^6; $S_{Fe}=0$) and two antiferromagnetically coupled π-radical ligands.
5) Finally, the diamagnetic octahedral complex **14** does not contain a low-spin ferrous ion, but rather a low-spin ferric ion[26] (d^5; $S_{Fe}=1/2$) that is antiferromagnetically coupled to a π-radical ligand $(L^{\bullet}_{TSC})^{2-}$.

Experimental Section

Quantum-chemical calculations: All DFT calculations were performed with the ORCA program package.[22]

The geometry optimizations of complexes were carried out at either the B3LYP[23,24] (or BP86) level[23,25] of DFT. The all-electron Gaussian basis sets were those developed by the Ahlrichs group.[26,27] For neutral **3**, **4**, **5**, **8**, and **9** and the monoanions **12** and **13** triple-ζ quality basis set TZV(P) with one set of polarization functions on the iron and on the atoms directly coordinated to the metal center were used.[27] For the carbon and hydrogen atoms, slightly smaller polarized split-valence SV(P) basis sets were used that were double-ζ quality in the valence region and contained a polarizing set of d-functions on the non-hydrogen atoms.[26] For the monoanions **1** and **2**, the TZV(P) basis set on all atoms was augmented by one set of diffuse functions for every valence shell by choosing an exponent equal to one third of the smallest exponent in the respective shell. Auxiliary basis sets used to expand the electron density in the resolution-of-the identity (RI) approach,[28] where applicable, were chosen to match the orbital basis.

Scalar relativistic corrections for **6**, **7**, **9**, and **10**, were included using the zeroth-order regular approximation (ZORA) method.[29]

The SCF calculations were tightly converged (1×10^{-8} E_h in energy, 1×10^{-7} E_h in the density change and 1×10^{-7} in maximum element of the DIIS error vector). The geometry search for all complexes was carried out in redundant internal coordinates without imposing symmetry constraints. In all cases the geometries were considered converged after the energy change was less than 5×10^{-6} E_h, the gradient norm and maximum gradient element were smaller than 1×10^{-4} $E_h Bohr^{-1}$ and 3×10^{-4} $E_h Bohr^{-1}$, respectively, and the root-mean square and maximum displacements of all atoms were smaller than 2×10^{-3} Bohr and 4×10^{-3} Bohr, respectively.

Corresponding,[22] canonical and quasi-restricted[30] orbitals and density plots were generated with Molekel.[31]

Nonrelativistic single-point calculations on the optimized geometries of iron complexes with the B3LYP functional were carried out in order to predict Mössbauer spectral parameters (isomer shifts and quadrupole splittings). These calculations employed the CP(PPP) basis set[32] for iron and the TZV(P) basis sets for N, S, C atoms.[28] The SV(P) basis sets were used for the remaining atoms. The Mössbauer isomer shifts were calculated from the computed electron densities at the iron centers as previously described.[8]

Throughout this paper we describe our computational results by using the broken-symmetry (BS) approach proposed by Ginsberg[33] and Noodleman.[34,35]

For many of the complexes studied in this work one can obtain several BS solutions to the spin-unrestricted Kohn–Sham equations. We adopted the following notation: the system was divided into two fragments. The notation BS(m,n) refers then to a broken-symmetry state with m unpaired spin-up electrons on fragment 1 and n unpaired spin-down electrons essentially localized on fragment 2. In most cases fragments 1 and 2 correspond to the metal and the ligand(s), respectively. Note that in this notation a standard high-spin open-shell solution would be written down as BS($m+n$,0). In general, the BS(m,n) notation refers to the initial guess to the wavefunction. The variational process does, however, have the freedom to converge to a solution of the form BS(m-n,0) in which effectively the n spin-down electrons pair with $n<m$ spin-up electrons on the partner fragment. Such a solution is then a standard $M_S \cong S=(m-n)/2$ spin-unrestricted Kohn–Sham solution. As explained elsewhere,[22] the nature of the solution is investigated from the corresponding orbital transformation (COT) which, from the corresponding orbital overlaps, displays whether the system is to be described as a spin-coupled or a closed-shell solution (see below).

The crystallographically determined structures have in some cases been simplified and truncated models have been used for the calculations: Complex **1** is the truncated form of $[Fe^{III}(L_{S,S})_2$(4-*tert*-butylpyridine)$]^-$, reference [9]; the structure of **2** was determined in reference [10]; the structures of **3** and **4** have not been determined; the structures of **5**, **10**, and **13** are the truncated forms of the *N*-phenyl-*o*-phenylenediamine derivatives in which the *N*-phenyl groups have been replaced by a hydrogen atom;[14] the structures of **6** and **7** were determined in references [21] and [10], respectively; the structure of **8** has not been determined; the structures of **9** and **11** are reported in references [16] and [17], respectively; complex **12** is a truncated form of the crystallographically characterized form in reference [15] in which the 4-*tert*-butyl groups are replaced by methyl groups; and **13** is a truncated form in which the original *N*-phenyl groups have been replaced by hydrogen atoms and the cyclohexyl group by a methyl group.[14]

Acknowledgement

We are grateful to the Fonds der Chemischen Industrie for financial support of this work.

[1] P. Chaudhuri, C. N. Verani, E. Bill, E. Bothe, T. Weyhermüller, K. Wieghardt, *J. Am. Chem. Soc.* **2001**, *123*, 2213.
[2] C. K. Jörgensen, *Oxidation Numbers and Oxidation States*, Springer, Heidelberg, **1969**.
[3] L. S. Hegedus, *Transition Metals in Synthesis of Complex Organic Molecules*, University Science Books, Mill Valley, **1994**, p. 3.
[4] a) B. Kirchner, F. Wennmohs, S. Ye, F. Neese, *Curr. Opin. Chem. Biol.* **2007**, *11*, 134; b) F. Neese, *J. Biol. Inorg. Chem.* **2006**, *11*, 702.
[5] F. Neese, *J. Phys. Chem. Solids* **2004**, *65*, 781.
[6] W. A. Goddard, T. H. Dunning, W. J. Hunt, P. J. Hay, *Acc. Chem. Res.* **1973**, *6*, 368.
[7] L. Noodleman, *J. Chem. Phys.* **1981**, *74*, 5737.
[8] S. Sinnecker, L. D. Slep, E. Bill, F. Neese, *Inorg. Chem.* **2005**, *44*, 2245.
[9] K. Ray, E. Bill, T. Weyhermüller, K. Wieghardt, *J. Am. Chem. Soc.* **2005**, *127*, 5641.
[10] S. Friedle, D. V. Partyka, M. V. Bennett, R. H. Holm, *Inorg. Chim. Acta* **2006**, *359*, 1427.

[11] M. Fettouhi, M. Morsy, A. Waheed, S. Golhen, L. Ouahab, J. P. Sutter, O. Kahn, N. Menendez, F. Varret, *Inorg. Chem.* **1999**, *38*, 4910.
[12] D. Sellmann, M. Geck, F. Knoch, G. Ritter, J. Dengler, *J. Am. Chem. Soc.* **1991**, *113*, 3819.
[13] a) T. Soda, Y. Kitagawa, T. Onishi, Y. Takano, Y. Shigeta, H. Nagao, Y. Yoshika, K. Yamaguchi, *Chem. Phys. Lett.* **2000**, *319*, 223; b) K. Yamaguchi, Y. Takahara, T. Fueno, *Applied Quantum Chemistry* (Ed.: V. H. Smith), Reidel, Dordrecht, **1986**, p. 155.
[14] K. Chlopek, E. Bill, T. Weyhermüller, K. Wieghardt, *Inorg. Chem.* **2005**, *44*, 7087.
[15] A. K. Patra, E. Bill, E. Bothe, K. Chlopek, F. Neese, T. Weyhermüller, K. Stobie, M. D. Ward, J. A. McCleverty, K. Wieghardt, *Inorg. Chem.* **2006**, *45*, 7877.
[16] D. Sellmann, S. Emig, F. W. Heinemann, *Angew. Chem.* **1997**, *109*, 1808; *Angew. Chem. Int. Ed. Engl.* **1997**, *36*, 1734.
[17] S. Blanchard, E. Bill, T. Weyhermüller, K. Wieghardt, *Inorg. Chem.* **2004**, *43*, 2324.
[18] M. D. Revenco, Yu. A. Simonov, N. I. Vyrtosu, N. V. Gerbeleu, P. N. Bourosh, B. K. Belski, K. M. Indrichian, *Zh. Neorg. Khim.* **1988**, *33*, 2049; *Russ. J. Inorg. Chem.* **1988**, *33*, 1168.
[19] M. D. Revenco, N. I. Vyrtosu, N. N. Gerbeleu, Yu. A. Simonov, P. N. Bourosh, A. N. Sobolev, *Zh. Neorg. Khim.* **1988**, *33*, 2353; *Russ. J. Inorg. Chem.* **1988**, *33*, 1343.
[20] N. N. Gerbeleu, Yu. A. Simonov, V. B. Arion, V. M. Leovac, K. I. Turta, K. M. Indrichan, D. I. Gradinaru, V. E. Zavodnik, T. I. Malinovskii, *Inorg. Chem.* **1992**, *31*, 3264.
[21] U. Knof, T. Weyhermüller, T. Wolter, K. Wieghardt, E. Bill, C. Butzlaff, A. X. Trautwein, *Angew. Chem.* **1993**, *105*, 1701; *Angew. Chem. Int. Ed. Engl.* **1993**, *32*, 1635.
[22] F. Neese, Orca—an ab initio, DFT and Semiempirical Electronic Structure Package, Version 2.4, Revision 36, Max-Planck-Institut für Bioanorganische Chemie, Mülheim (Germany), May 2005.
[23] A. D. Becke, *J. Chem. Phys.* **1986**, *84*, 4524.
[24] a) A. D. Becke, *J. Chem. Phys.* **1993**, *98*, 5648; b) C. T. Lee, W. T. Yang, R. G. Parr, *Phys. Rev. B* **1988**, *37*, 785.
[25] a) J. P. Perdew, W. Yue, *Phys. Rev. B* **1986**, *33*, 8800; b) J. P. Perdew, *Phys. Rev. B* **1986**, *33*, 8822.
[26] A. Schäfer, H. Horn, R. Ahlrichs, *J. Chem. Phys.* **1992**, *97*, 2571.
[27] A. Schäfer, C. Huber, R. Ahlrichs, *J. Chem. Phys.* **1994**, *100*, 5829.
[28] a) K. Eichkorn, F. Weigend, O. Treutler, R. Ahlrichs, *Theor. Chem. Acc.* **1997**, *97*, 119; b) K. Eichkorn, O. Treutler, H. Ohm, M. Haser, R. Ahlrichs, *Chem. Phys. Lett.* **1995**, *242*, 652; c) K. Eichkorn, O. Treutler, H. Ohm, M. Haser, R. Ahlrichs, *Chem. Phys. Lett.* **1995**, *240*, 283.
[29] a) C. van Wüllen, *J. Chem. Phys.* **1998**, *109*, 392; b) E. van Lenthe, E. J. Baerends, J. G. Snijders, *J. Chem. Phys.* **1993**, *99*, 4597.
[30] a) J. C. Schöneboom, F. Neese, W. Thiel, *J. Am. Chem. Soc.* **2005**, *127*, 5840; b) F. Neese, *J. Phys. Chem. Solids* **2004**, 65, 781.
[31] Molekel, Advanced Interactive 3D-Graphics for Molecular Sciences, available under http:www.cscs.ch/molekel/.
[32] F. Neese, *Inorg. Chim. Acta* **2002**, *337*, 181.
[33] A. P. Ginsberg, *J. Am. Chem. Soc.* **1980**, *102*, 111.
[34] L. Noodleman, C. Y. Peng, D. A. Case, J. M. Mouesca, *Coord. Chem. Rev.* **1995**, *144*, 199.
[35] a) L. Noodleman, D. A. Case, A. Aizman, *J. Am. Chem. Soc.* **1988**, *110*, 1001; b) L. Noodleman, E. R. Davison, *Chem. Phys.* **1986**, *109*, 131; c) L. Noodleman, J. G. Norman, J. H. Osborne, A. Aizman, D. A. Case, *J. Am. Chem. Soc.* **1985**, *107*, 3418; d) L. Noodleman, *J. Chem. Phys.* **1981**, *74*, 5737.

Received: June 13, 2007
Published online: September 11, 2007

